Journal of
Marine Science and Engineering

MDPI

Article

On the Fate of Floating Marine Debris Carried to the Sea through the Main Rivers of Indonesia

Delphine Dobler [1], Christophe Maes [1,*], Elodie Martinez [1], Rinny Rahmania [2], Budhi Gunadharma Gautama [2], Aulia Riza Farhan [3] and Edmond Dounias [4]

[1] LOPS-Laboratory of Ocean Physics and Satellite Remote Sensing, IRD-French National Research Institute for Sustainable Development, 29280 Plouzané, France; delphine.emilie.dobler@protonmail.com (D.D.); elodie.martinez@ird.fr (E.M.)
[2] National Research and Innovation Agency, Gedung B.J. Habibie, Jl. M.H. Thamrin No. 8, Jakarta Pusat 10340, Indonesia; rinny.rahmania@brin.go.id (R.R.); budh008@brin.go.id (B.G.G.)
[3] Marine and Fisheries Surveillance Systems, Ministry of Marine Affairs and Fisheries, Jakarta Pusat 10340, Indonesia; riza.farhan@kkp.go.id
[4] CEFE (Centre d'Écologie Fonctionnelle et Évolutive), Université de Montpellier, CNRS, EPHE, IRD, 1919, Route de Mende, 34293 Montpellier, France; edmond.dounias@ird.fr
* Correspondence: christophe.maes@ird.fr

Abstract: Plastic debris has become an acute marine pollution concern worldwide in modern times. Indonesia is particularly impacted because of its high population density, heavy rainfall rate and numerous coastlines. A Lagrangian analysis was performed to simulate the fate of fictive marine debris drifting along surface currents, including tides and Stokes drift. The fictive particles were released according to the discharge rate of 21 Indonesian rivers and advected over 4 years. Most of the particles were stranded along Indonesian coasts (60%), before 6 months had elapsed (84%) and within a range of 1000 km (76%). The time variability exhibited two seasonal peaks, one centered on January-February and one on June-July, consistent with in situ observations. However, the results underline the complexity of performing direct comparisons between in situ observations and numerical simulations for stranded waste due to limited measurements and the heterogeneity of field methods and protocols.

Keywords: marine debris; plastics dispersion; numerical modeling; strandings; Indonesian seas

Citation: Dobler, D.; Maes, C.; Martinez, E.; Rahmania, R.; Gautama, B.G.; Farhan, A.R.; Dounias, E. On the Fate of Floating Marine Debris Carried to the Sea through the Main Rivers of Indonesia. *J. Mar. Sci. Eng.* **2022**, *10*, 1009. https://doi.org/10.3390/jmse10081009

Academic Editors: Ali Belmadani and Jean-Philippe Maréchal

Received: 10 June 2022
Accepted: 20 July 2022
Published: 23 July 2022

1. Introduction

Plastic pollution is a major issue in our modern societies. This pollution began in the 1950s with the rise of the plastic age, and plastic production reached up to 368 million metric tons (MT) in 2019 and is increasing by an average of 16 MT every year [1]. A percentage of this production ends up at sea, but assessing its volume and weight remains a complicated task. Estimations were made in [2,3] using indirect information such as waste management data, population density, hydrology and the economic status of the country in question. These studies estimated that between 1.15 and 12.7 MT of plastics enter the ocean each year. Whatever its total global amount and size spectrum (macro, micro and nano), marine plastic debris has significant impacts. This pollution seriously harms marine biota; organisms perish after ingestion, entanglement or suffocation [4–6]. It also deteriorates natural ecosystems, such as coral reefs, and affects economically important marine activities, such as shipping, fishing, aquaculture, tourism and recreation [4,7,8].

Inland sources are often estimated to represent the major contributors to plastic pollution at sea [9], and their associated plastic waste mainly enters the ocean through rivers [3] and global wastewater influent [10]. Once at sea, this pollution is dispersed by currents and affected by biofouling. Some waste is advected over long distances before reaching one of the five main accumulation areas located inside the subtropical gyres [11–14]. Some

waste degrades into smaller pieces (either primary or secondary microplastics, depending on the product type) due to thermal, chemical and physical disintegration and/or is subject to biofouling [15] and sinks [16], while some finally strands [17,18]. While it is necessary to estimate the quantity and the spatio-temporal distribution of each scenario (i.e., subtropical gyre convergence, sinking or stranding) to implement appropriate mitigation actions, it is noteworthy that these final estimates highly depend on the pollution source scenario [19].

Based on the aforementioned indirect information, Indonesia is ranked as the second-most-polluting country [2]. This rank should be viewed in a nuanced manner as the information used in its calculation is subject to uncertainties [20]. Nonetheless, Indonesia is particularly impacted by marine plastic pollution as a consequence of its high population density, especially that of Java, one of the largest megalopolises in the world (with a population of 145 million people [21]); its high level of rainfall (320 mm/y [22]); and its jagged shoreline that includes more than 13,000 islands and many narrow straits [23]. In this context, one Indonesian presidential decree was adopted in 2017 and another in 2018; both addressed waste and marine debris management and were followed by policy plans [24]. The present study aims to support these initiatives by providing a better understanding of marine debris surface pathways and stranding locations in this region.

The Indonesian region spans the Equator and is a unique pathway between the tropical Pacific and Indian oceans (Figure 1). It is the scene of intensive marine traffic, which is amplified by the modern Chinese Silk Road; it also plays an important role in the transport of water masses and is subject to intense ocean dynamics. For instance, surface Stokes drift contributes to the surface drift of floating debris [25,26], while equatorially trapped waves followed by Kelvin coastal waves [27] may locally impact currents [28] and thus debris dispersion and/or accumulation. Tidal currents are locally very strong and complex [29,30]. Extreme events, such as earthquakes and associated tsunamis [31] and typhoons (mainly poleward of 8° of latitude [32]), also occur in this region. In addition, the monsoon regime reverses surface currents while El-Nino-Southern-Oscillation (ENSO) and climatic change strongly influence current intensity and rainfall [33,34].

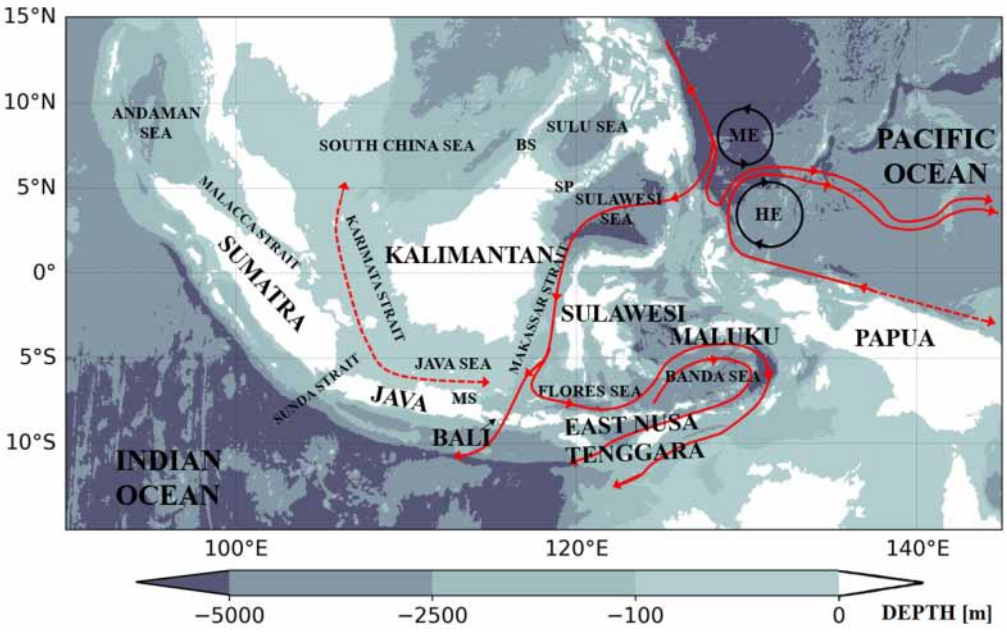

Figure 1. Indonesian region bathymetry, main islands and currents. Shades of blue-gray illustrate the bathymetry (in meters). Red lines and arrows illustrate the Indonesian throughflow. Dashed lines illustrate two currents reversing with the monsoons (southeastward during the North Monsoon centered on July and August and northwestward during the South Monsoon centered on January and February). Acronyms: ME, Mindanao Eddy; HE, Halmahera Eddy; BS: Balabac Strait; SP: Sibutu Passage; MS, Madura Strait.

To understand the trajectories and fates of floating marine debris, a Lagrangian numerical experiment was performed using surface currents from a 1/12° ocean general circulation model (OGCM). We investigated the impact of surface current dynamics and source scenarios on the drift of floating marine debris in the Indonesian area. To increase the awareness of Indonesian institutions, an atlas mapping marine debris stranding along Indonesian coasts was provided to the Indonesian government to help in determining a mitigation strategy to reduce this pollution [35]. The present study is mainly based on the methodology and results presented in detail in this atlas. In the present study, we investigated more thoroughly the seasonal variability in debris stranding, and we compared our results from numerical modeling to two sets of field observations. The contributions and difficulties of such a comparison between field measurements and numerical simulations are discussed herein. One important point to keep in mind is that the goal of the present study is to focus not on a particular type of product or plastic but rather on the fate of floating material under the influence of ocean dynamics.

2. Materials and Methods

2.1. Materials

2.1.1. Surface Oceanic Currents

We used the Surface Merged Ocean Currents (SMOC) product from Mercator, which sums the surface currents from the NEMO ocean general circulation model (OGCM) that assimilates both in situ and remote-sensed data with tide and wave (i.e., Stokes drift) components [36]. More specifically, the NEMO OGCM uses NEMO 3.1 in a PSY4V3R1 configuration. It considers atmospheric forcings from ECMWF and freshwater inputs from rivers using both observations of coastal runoff (including 100 major rivers from [37]) and a model of streamflow (the community land model version 3); it also assimilates data on remote-sensed sea surface temperatures, sea-ice concentrations, sea level anomalies, in situ temperature and salinity profiles (above 2000 m) and WOA climatology below 2000 m. The choice of the SMOC product was driven by the known significant impact of the Stokes drift on particles' trajectories [25,26] and by the large tidal influence in the region [29,30]. The SMOC product is distributed by the Copernicus Marine Service (CMEMS) and provides surface currents interpolated on a regular 1/12° grid at an hourly frequency beginning 1 April 2016. The present study considered the period ranging from 1 April 2016 to 30 April 2020. More details are available on the CMEMS website [36] and in the technical atlas [35]. The accuracy of models, with respect to Lagrangian experiments, is often estimated by computing separation distances or derived quantities with observations [38,39]. According to the quality document of CMEMS (see the documentation section of [36]), using the SMOC product instead of the OGCM surface currents only globally improves by 18.7% (i.e., 36.5 km compared to 44.9 km) the separation distance at three days between simulated trajectories and real trajectories from undrogued drifters provided by the Global Drifting Program (GDP) over a 2-yr period (1 April 2016 to 1 April 2018). We re-computed the same diagnostics for the period of interest, and we found a similar improvement. For the Indonesian region, as defined by [90, 145] °E × [−25, 35] °N and during a 4-year period (1 April 2016 to 30 April 2020), a total of 384 GDP drifters were found with 156,970 available positions when their drogues were lost. For this set of positions, the improvement reached 11.1% at three days, with an average separation of 45.5 km using the SMOC product as compared to 51.2 km using the OGCM surface current data only. However, it should be kept in mind that only a few drifters flow across the Indonesian seas that remain largely undersampled (1 in the Java Sea and 4 in the Sulawesi Sea).

2.1.2. River Discharge

Inland waste mainly enters oceans through river systems. Consequently, relationships exist between the input rate of waste into the ocean and river discharge. The modeling of this relationship is detailed below in the Methods section. River discharges were estimated using the Global Flood Awareness System dataset provided by the Copernicus Emergency

Management Service [40]. This system combines a hydrological model and in situ measurements. The discharge rates of Indonesian rivers range from 50,000 to 150,000 m^3/s, with a strong seasonal signal. For instance, a dry season can be observed on Java and the surrounding islands, whereas a more permanent flux characterizes the freshwater river flux on Kalimantan (Figure 2).

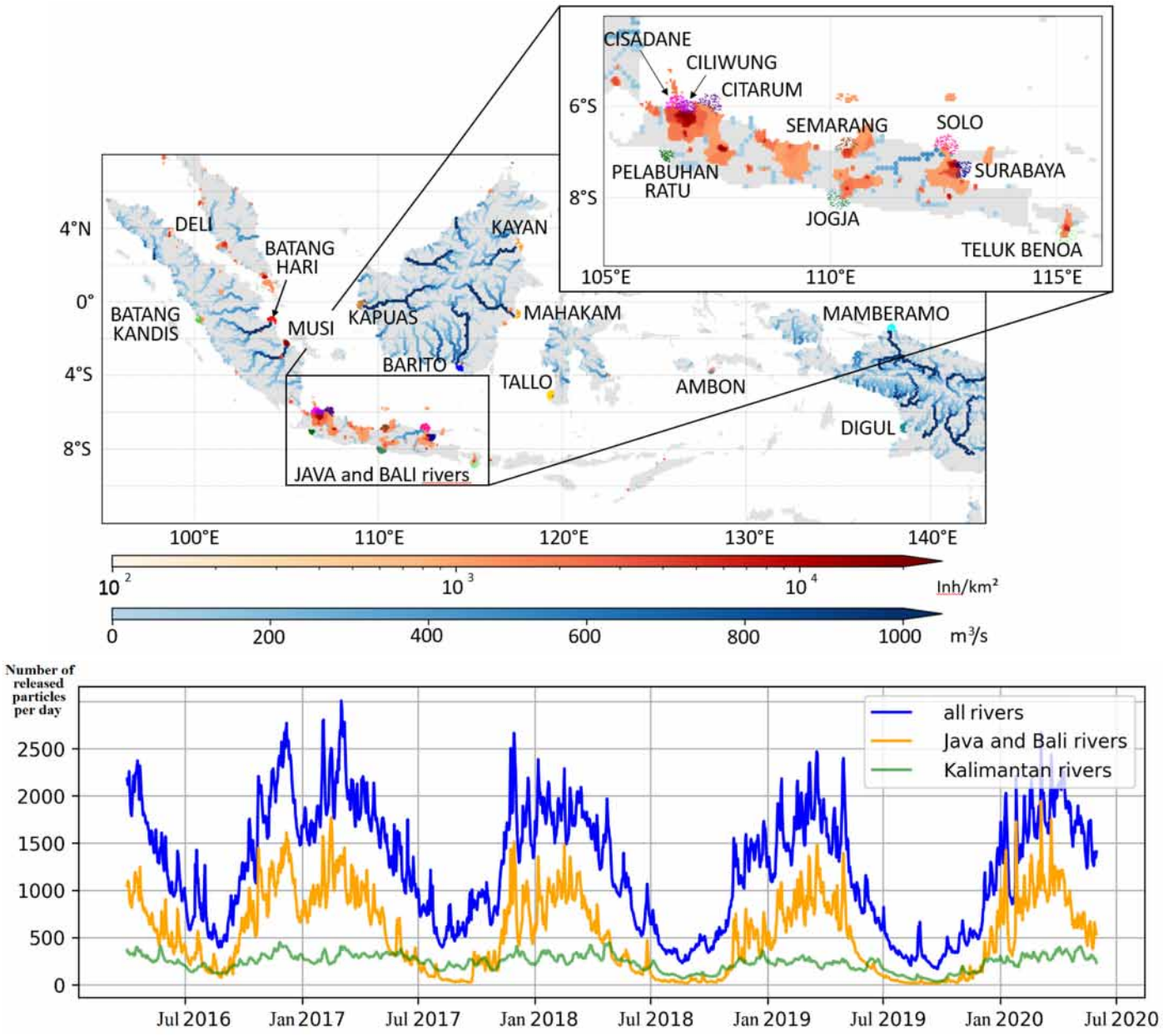

Figure 2. Spatial and temporal characteristics of the source scenario. Upper panel: names and locations of the 21 rivers selected to release particles in the simulation. River discharges [m^3/s] are indicated in shades of blue and population density [inhabitant/km^2] in shades of orange. Colored dots indicate the particle release position on the first day of the simulation. The colors differentiate the riverine origins. See [35] for detailed coordinates of river mouths. Lower panel: time series of the sum of released particles for all 21 rivers (blue line), the 9 rivers of the islands of Java and Bali (orange line) and the 4 rivers from Kalimantan (green line). The daily number of released particles linearly follows the river discharge evolution. This relationship is detailed in Section 2.2.2 on the "river source scenario".

2.1.3. Population Density

Population density was also considered as a qualitative parameter when building the source scenario. This information was extracted from data for the year 2015 in the NASA Socioeconomic Data and Applications Center dataset [21]. Java Island is the most densely populated region, with more than 1000 inhabitants per square kilometer.

2.1.4. Waste Observations

Two datasets of waste observations were considered for comparison with our model results.

The first dataset was extracted from visual surveys provided in Table 2 of [41]. It is hereafter referred to as "GS". The authors of GS performed counts of floating debris by visual surveys in the coastal waters of three sites of interest: the Manta Bay close to Bali, Karang Makassar in the Komodo National Park close to East Nusa Tenggara and, finally, Pantai Bentar along the East Java coast south of the Madura Strait. These surveys were conducted between 2016 and 2018 and, for each site, the average counts and standard error results for the wet season (January to May) and dry season (August to October) were provided. A scientific protocol was similarly applied at each site to produce comparable field data.

The second dataset was derived from the work Dr. Sapta Putra Ginting and collaborators and was presented at the APEC Meeting of Bali in February 2020 [42,43] (Sapta Putra Ginting, personal communication). It is hereafter referred to as "PS". The authors of PS performed 26 beach cleaning sessions between 2017 and 2019 and recorded the weight of collected waste in metric tons. Seventeen beach cleaning sessions located on Java, Bali and East Nusa Tenggara were retained to be consistent with the locations from GS. It is noteworthy that no standard protocol was applied in this case and that the cleaned areas and sampling durations differed for each site and were not recorded. Furthermore, probable previous cleaning sessions conducted by local authorities or civil society actors were also not taken into consideration. However, these observations remain highly valuable because they cover a wide region and coincide with the period of our simulation.

2.2. Methods

2.2.1. Lagrangian Drift

To assess waste stranding and dispersion in the Indonesian region, a Lagrangian simulation was performed. The Lagrangian point of view allows multiple analyses of particle trajectories (e.g., [44]), including covered distance, drift time, stranding location, connectivity patterns between regions, backward analyses and probabilistic analyses. We used the Lagrangian software package Ariane, originally developed by B. Blanke and S. Raynaud [45], available at www.univ-brest.fr/lpo/ariane (accessed on 9 June 2022); it was released by the Laboratory of Ocean Physics and Satellite Remote Sensing (LOPS, France) and has been maintained since 2006. Ariane software computes trajectories from a 1D linear formulation using input 3D current fields and builds water mass transport diagnostics. More specifically, on the latter point, Ariane ensures the conservation of mass attributed to the elementary particle flowing through each numerical cell. The implication of this conservation of mass means that it avoids the necessity of considering random-walk modeling or any type of diffusion in addition to the trajectory computation. The present approach thus represents a purely kinematic method associated with the stirring conditions of the current (other methods and codes are discussed by [44]).

In this study, the trajectories of surface floating particles were advected using SMOC currents in the Indonesian region, as defined by $[90, 145]^\circ$ E $\times$ $[-25, 35]^\circ$ N and during a 4-year period (1 April 2016 to 30 April 2020). Only surface pollution was investigated, and we assumed no emerged part (the windage, also known as the leeway drift, was not assessed in this study). Accordingly, numerical particles were forced to remain in the surface layer by prescribing a null vertical velocity in the Ariane software package.

2.2.2. River Source Scenario

According to the situation described recently by [46], namely that "for relatively short rivers with high population densities close to the river and the coast, such as found in the Philippines and Indonesia, plastics are more likely to be emitted into the ocean", we based our approach on the contributions of the most important rivers. A total of 21 river mouths were selected to release particles (upper panel of Figure 2). These rivers were selected because they are well-known plastic waste pollution sources (e.g., a communication from the Indonesian Ministry of Marine Affairs and Fisheries and from the Ocean Cleanup project stated that it concerned the Cisadane, Ciliwung, Semarang, Surabaya, Solo, Teluk Benoa, Jogja, Palabuhan Ratu, Musi, Kapuas, Tallo and Ambon rivers), and/or because there are settlements on their banks with high population density (this includes the Citarum, Deli, Batang Kandis, Batang Hari, Barito, Mahakam and Kayan rivers) and/or because their discharge volume is large (this includes the Digul and Mamberamo rivers). Among these 21 rivers, 8 are located on Java, 1 on Bali, 4 on Kalimantan, 4 on Sumatra, 1 on Sulawesi, 1 on Maluku and 2 on Papua. We decided to release almost 2 million particles for the whole simulation. This large number was chosen as a balance between statistical needs and computational constraints. These particles were distributed in time and space. Particles were released every day at midnight within a 30 km range around the river mouth (colored dots on the upper panel of Figure 2). This release distance was chosen after an analysis of sea surface salinity (SSS) gradients to estimate the river plume mean extension (not shown). Without any preliminary information on the rivers' relative levels of pollution, the same total number of particles (90,000) was released over the 4 years of the simulation for each river; the daily release for each river was linearly weighted by its respective daily discharge (lower panel of Figure 2). This linear relationship was chosen in the absence of a more accurate field observation of this relationship because it represents the simplest relationship that could exist between discharge and debris inputs. It was mathematically written as follows: $N(D,R) = round(N_t(R) \times \frac{Dis(D,R)}{\sum_D Dis(D,R)})$, with $N(D,R)$ being the number of released particles for river R on day D, $N_t(R)$ the total number of particles released for the river R (set to 90,000 particles here), $Dis(D,R)$, the discharge of the river R for day D and $\sum_D Dis(D,R)$ the sum over the period of the daily discharge for river R. It is noteworthy that rivers on the islands of Java and Bali have clear seasonal signals, with peaks of 1500 released particles per day (530 ± 410) during the wet season and almost no released particles during the dry season. This seasonality is not as marked for other rivers; for instance, the average daily release of particles was 240 ± 90 for Kalimantan rivers.

2.2.3. Definition of Debris Stranding

Particular attention was devoted to the definition of stranding. The stranding of floating debris is a multi-factorial process and remains complicated to parameterize [47]. It depends on several factors, such as coastal currents, tidal conditions, beach types, wind and waves, sand burying and back release [48]. Coastal processes are not well resolved in a $1/12^\circ$ simulation, and the numerical coast was quite coarse and lacked bay and cape representation in the Indonesian region. Considering these limitations, the stranding definition was kept as simple as possible while remaining consistent with the modeling: a particle was considered stranded when it drifted within 9 m (i.e., 10^{-3} times the grid resolution) of the numerical coastline. This threshold value was chosen after a series of sensitivity tests (see [35] for details). The main constraint was to remain below the grid resolution to stay consistent with the numerical representation of straits.

To assess the spatial variability in strandings, the Indonesian region was divided into several subzones. Divisions followed a political and/or geographical pattern. For instance, Java Island was divided into two subzones: the North Java region for the coastline facing the Java Sea and the South Java region for the coastline facing the Indian Ocean. Borneo Island was divided into three subzones: the Malaysian part in the north-west and two subzones for the Indonesian part. The first was the south and south-west Kalimantan coast

facing the Karimata Strait and the second was the Java Sea and the east Kalimantan coast facing the Makassar Strait. The delimitation of all the subzones is further detailed in [35].

2.2.4. Waste Observations and Simulation Comparisons

Several methods can be used to assess the performance of waste pathway models and stranding estimates. In this study, the waste count observations described in GS and PS were compared to the simulated strandings.

It is noteworthy that the GS observations did not correspond to stranding observations but to visually identifiable accumulations of floating materials in zones very close to the coast (less than 500 m). However, we decided to include this type of field observations in our comparison with simulated strandings, firstly because studies eligible for comparison with simulated strandings in the Indonesian region are very scarce and, secondly, because this visual study was performed very close to the coast where we can assume that the amount of at-sea debris correlated with the number of strandings along nearby coasts. It is also noteworthy that beach cleaning session data from PS are also a best-we-have proxy for data on strandings; collected waste may come not only from offshore but also from land or beach activity (commercial, recreational, etc.). Here again, we decided to include this study because of the scarcity of eligible studies.

To perform this comparison, we summed the simulated particles that were stranded for a given period before the relevant site's observation date and within a given distance of the site's location. For both waste observations datasets, the threshold distance was set to 20 km. This roughly corresponds to the length of two grid cells in the SMOC model grid. On the other hand, time thresholds were adjusted to the particularities of each dataset. The cleaning sessions that yielded the PS data only lasted one day, and strandings that occurred in the 7 days prior to the cleaning session date were considered. This 7-day limit corresponded to an approximative period of debris accumulation that occurred before the cleaning session. In contrast, GS provided data gathered during periods of 1 to 3 months in the wet or dry seasons of the years 2016 to 2018. Their Komodo site was not sampled in 2018, and their Pentai Bentar site was only sampled during the 2017 wet season. Considering these limitations, the simulated strandings were summed when they occur in the 60 days prior to the end of the 2017 wet or dry seasons. An error estimate was also computed and corresponds to the 5th and the 95th percentiles of the values obtained when taking into account small changes in the site location (within 10 km for both datasets) and date (within minus 30 days for GS and within plus or minus 7 days for PS).

3. Results

3.1. Main Dispersion Features

After simulating a 4-year period (from 1 April 2016 to 30 April 2020), 10% of the released particles still drifted on the ocean surface within the Indonesian region (Figure 3). These particles were almost all located within a latitudinal band extending from 15° S to 12° N. They were abundant in the internal seas, such as the Sulawesi, Java, Flores and Banda seas, and also along the Malacca, Karimata and Makassar straits and in the southwestern part of the South China Sea.

During the same period, 30% of particles exited the Indonesian region through the lateral open boundaries. Most of them (67%) exited through the south Indian Ocean, mostly during the months from July to December, and followed a wide pathway extending from 15° S to 5° S along 90° E. A few of them (20%) exited through the Malacca Strait into the north Indian Ocean, mostly from January to June. The remaining particles (13%) exited into the Pacific Ocean. Half of them exited into the north Pacific Ocean, advected by the Pacific North Equatorial Counter Current, mostly from July to December. Half of them exited into the south Pacific Ocean by flowing along the New Guinea Coastal Current, mostly from November to May.

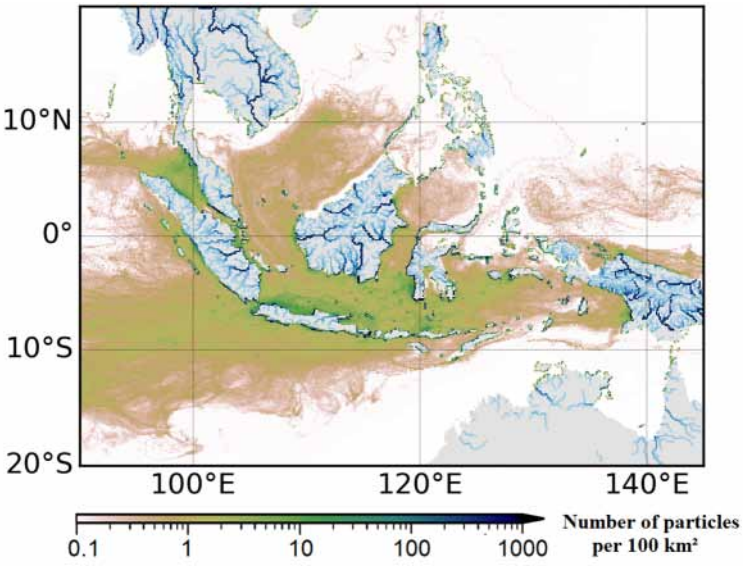

Figure 3. Time average number of simulated particles per 100 km^2 over the last year of simulation (1 of April 2019 to 1 of April 2020).

Finally, the majority of the released particles (60%) stranded within the Indonesian region (Figure 4). Strandings mainly occurred along Indonesian coasts (92%), which is consistent with both the observed particle dispersion (within a latitudinal band extending from 15° S to 12° N) and the source scenario (Indonesian riverine sources only). The upper panel of Figure 4 highlights locations with a high number of strandings. The largest number of strandings were located along the northern and southern coasts of Java (80 particles/km), followed by West Sulawesi (70 particles/km) and Bali (65 particles/km). Further details regarding stranding rates for each subzone can be found in Table 3 of the atlas [35]. The lower panel of Figure 4 focuses on the islands of Java and Bali and shows finer categories for the stranding amounts. High rates of strandings (red and blue disks) were mostly located close to a riverine source (illustrated by a white star). These results suggest that stranding occurs rapidly close to the source region.

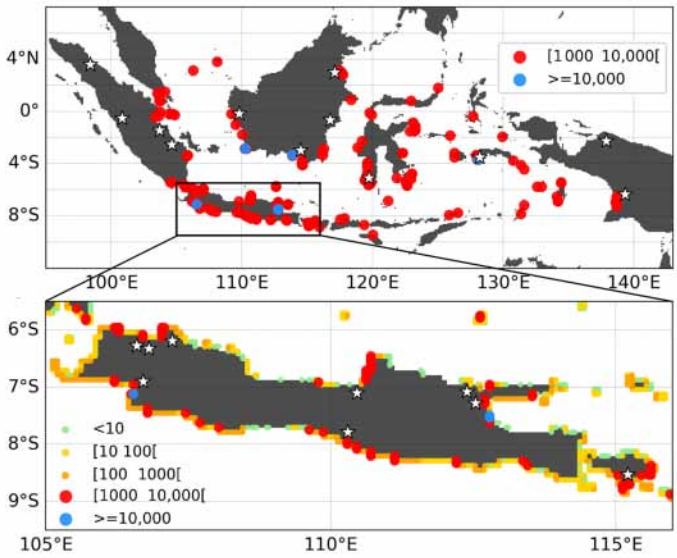

Figure 4. Locations of stranded particles along Indonesian coasts. White stars indicate the riverine sources. The upper panel shows locations where more than 1000 and more than 10,000 particles were stranded on the same coastal numerical segment 5 km in length. The lower panel focuses on the islands of Java and Bali.

3.2. Spatio-Temporal Variability in Debris Stranding

Our results showed that floating marine debris stranded at any time of the year and originated from all riverine sources. Nonetheless, some variability was observed in terms of sources, maximum stranding period and location (Figure 5). The contribution of a given riverine source to the total number of stranded particles over the 4-year simulation fluctuated by a ratio of 3, for instance, from 1.9% for the Deli River to 6.5% for the Ambon River. Riverine sources located in enclosed bays contributed more (e.g., the Ambon and Surabaya rivers were among the three most-contributing rivers).

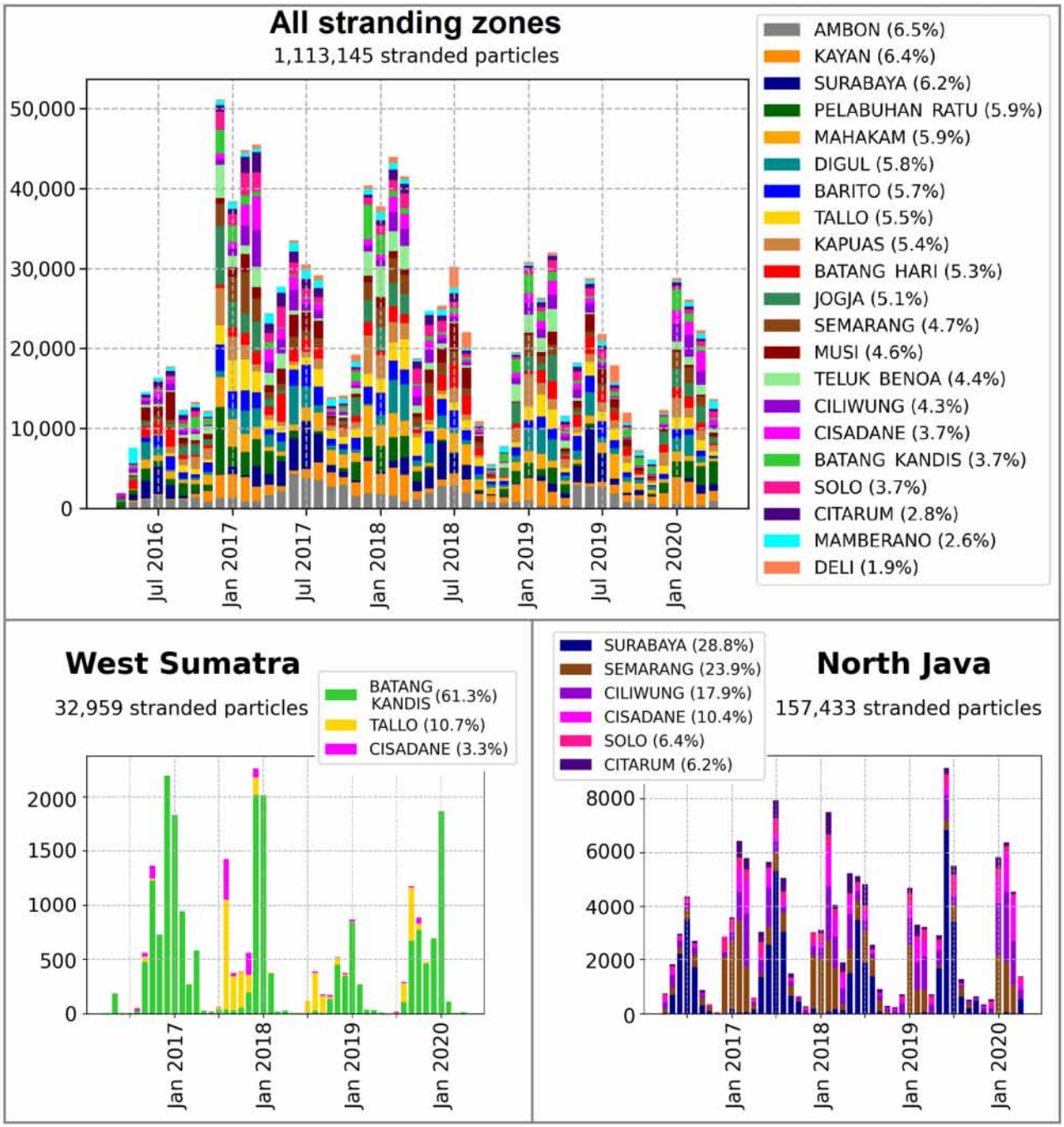

Figure 5. Time series of particle strandings along the coasts of the entire region (**upper panel**), West Sumatra (**lower left panel**) and North Java (**lower right panel**). Note that the ordinate axis range differs between the three panels.

On average, strandings showed seasonality, with two peaks: one centered on January-February and one on June-July. The seasonality of strandings was not homogeneous throughout the region. Half of the regional subzones, such as West Sumatra and North Sulawesi, only peaked once. This peak generally occurred during January, February, March, July or August. Some subzones did not show any particular peak season (for instance, North Papua, East Nusa Tenggara, and East Sumatra). On the other hand, strandings on East Sulawesi, South Kalimantan, East Kalimantan and North Java peaked twice. In particular, the peaks for strandings on North Java were phased with the general pattern. This behavior is consistent with the fact that this subzone contributed the most to the total number of strandings. Inter-annual variations were also observed, with more strandings occurring during the years 2017 and 2018. However, the 4-year time series was too short to allow any confident association with ENSO or the Indian Ocean Dipole (IOD).

Most particles seemed to strand close to their release position (lower panel of Figure 5). For instance, along the North Java coasts, 94% of stranded particles originated from one of the six rivers of North Java, whereas the remaining 6% originated from remote sources. Strandings that occurred along the West Sumatra coast nicely illustrate the different types of connectivity (Figure 6). Most of the stranded particles (63%) originated from the local Batang Kandis and Deli rivers (upper left panel of Figure 6), but a significant number of strandings (13%) originated from the more remote Tallo and Ambon rivers (upper right and lower panels of Figure 6). These remote contributions can follow direct or indirect pathways. Indirect pathways illustrate the connectivity existing between remote places, for instance, between the southeastern tip of Sumatra and the South China Sea, the Sulu Sea, and the Makassar Strait (upper right panel of Figure 6) and between Sumatra and the Mindanao Eddy in the Pacific Ocean, the Sulawesi Sea, and the Molucca region (lower panel of Figure 6).

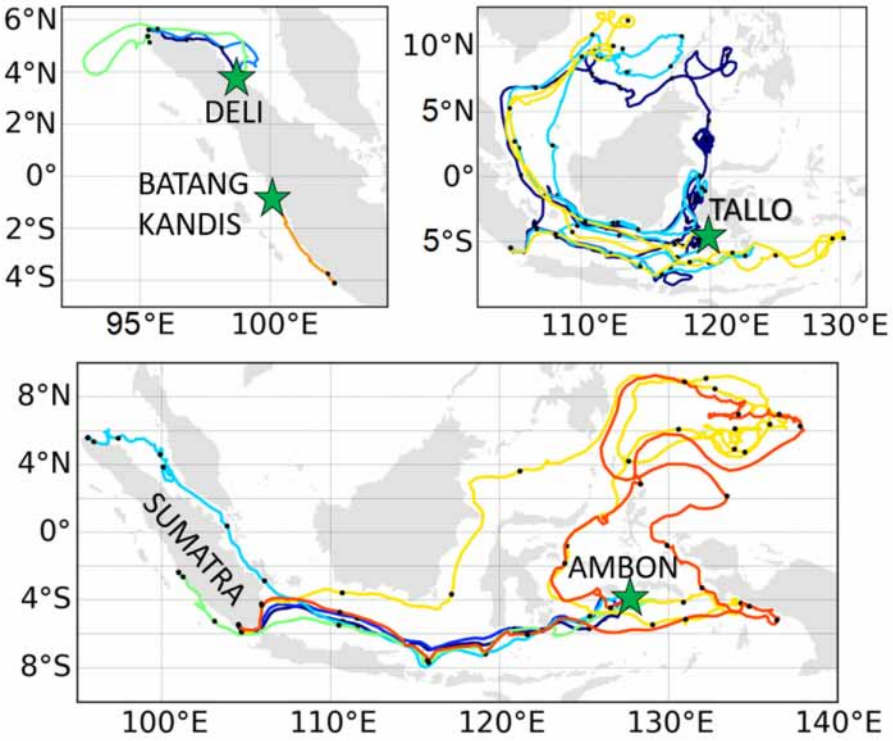

Figure 6. Examples of trajectories (in differentcolors per particle) of particle stranding along the western coast of Sumatra. Trajectory origins are indicated by green stars associated with the respective names of the rivers. Successive black dots illustrate 30-day intervals along each trajectory. The upper left panel shows the stranding location of locally released particles. The other two panels illustrate trajectories of particles with remote origins and long drifts.

All of these examples qualitatively describe the different types of existing connectivity. To quantify how many strandings originate from local versus remote sources, statistics regarding stranding age (the number of days between the release date and the stranding date) and the distance between particles' initial release positions and stranding locations were systematically assessed (Figure 7).

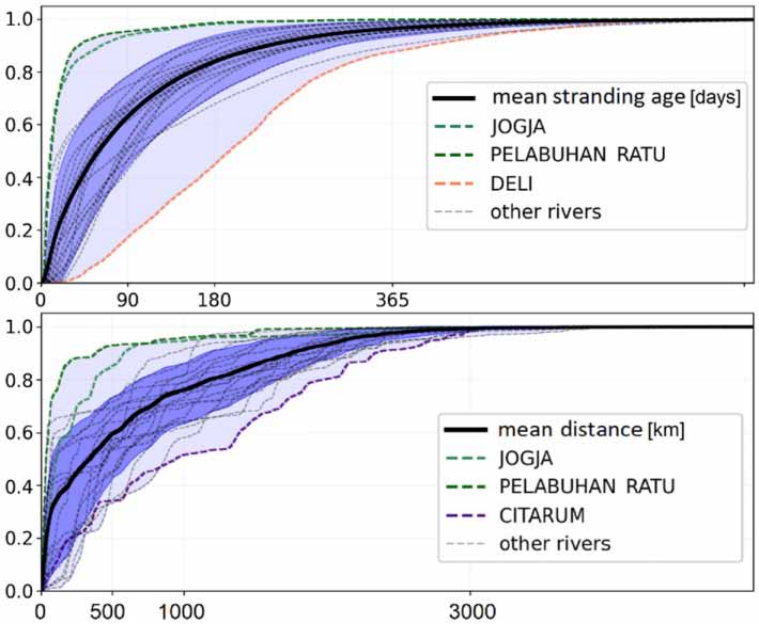

Figure 7. Upper panel: normalized cumulative sum of stranding ages for particles released from 21 Indonesian rivers. Bottom panel: normalized cumulative sum of the distances between particles' initial locations and stranding locations. For both panels, the thick black line represents the normalized cumulative sum for all stranded particles, regardless of the riverine origin. The dashed lines correspond to normalized cumulative sums of stranded particles originating from a given riverine source. The extreme patterns displayed by the Jogja, Pelabuhan Ratu, Deli and Citarum rivers are highlighted with colored dashed lines. The dark purple shading corresponds to the standard deviation with respect to the riverine source. The light purple shading highlights the minimum and maximum values.

Temporally, most particles stranded quickly: 63% before 3 months, 84% before 6 months and 96% before one year. Three riverine sources stood out from the general pattern: particles from the Jogja and Palabuhan Ratu rivers were the fastest to strand, being advected by the eastward Java coastal current toward the southern coast of Java Island. On the other hand, particles from the Deli River, located on the northeastern coast of Sumatra, had the longest drift before stranding: only 15% stranded before 3 months and 40% before 6 months. Particles that stranded after 6 months tended to recirculate in eddies located in the northern entrance of the Malacca Strait, on the northern tip of Sumatra and in the Andaman Sea between Great Nicobar Island and the Sunda Shelf. Consistently, the mean residence time was two times greater in the northern entrance of the Malacca Strait (30 days in a 200-km radius) than in the Andaman Sea, near the Indian Ocean or in the Java Sea (15 days on average).

Spatially, most particles stranded close to their riverine source, with 60% stranding less than 500 km away and 76% less than 1000 km away. Consistent with the data for particle stranding age, particles from the Jogja and Pelabuhan Ratu rivers stranded the closest to their source. On the other hand, the particles that stranded the farthest from their source were from the Citarum River (51% stranded within 1000 km from the source). It is noteworthy that the nearby Cisadane and Ciliwung rivers behaved according to the average (63% and 71% stranded within 1000 km, respectively). Despite their closeness (77 km apart), the Citarum River mouth is located on a cape, whereas the Cisadane and Ciliwung river

mouths are located inside a bay. More particles from the Cisadane and Ciliwung rivers stranded along the Javanese coasts (54% and 64%, respectively) than particles from the Citarum River (36%). Conversely, more particles from the Citarum River stranded along the coasts of the islands of Sulawesi and Maluku (33%) than particles from the Cisadane and Ciliwung rivers (25% and 20%, respectively). These observations suggest that particles from the Citarum River were more easily entrained by the eastward current flowing in the Java Sea from October to April because of the river mouth's location on a cape.

3.3. Comparison between Simulation and Field Observations

To assess the performance of our simulation, obtained stranding rates were compared to field observations from GS and PS. The comparison was limited to the islands of Java, Bali and East Nusa Tenggara because this geographical zone corresponds to an area of particular interest for local authorities and stakeholders, partly because of tourism-related activities and income.

Debris counts from GS contrasted between the wet and the dry seasons (left panel of Figure 8) with, on average, 30 times more debris at the Bali and East Nusa Tenggara sites during the wet season (20,122 vs. 605 items/km^2 during the dry season). This contrasting pattern was well reproduced in our simulation, with, on average, 60 times more simulated strandings during the wet season than during the dry season. It is noteworthy that our results, which were based on numerical simulation, were sensitive to slight changes in the location and date of the sites, as illustrated by the error bars. Despite this sensitivity, the number of simulated strandings remained greater during the wet season than during the dry season. The behavior at site S704 was singular: the survey was performed during the wet season with potential pollution from the nearby Surabaya River, but very little floating waste was observed at this location. Accordingly, in our simulation, no stranding occurred along this coast south of the Madura Strait (Figures 4 and 8). The coastline shape and the main current zonal direction may explain this singularity: most particles from the Surabaya River are directly advected eastward out of the Madura Strait.

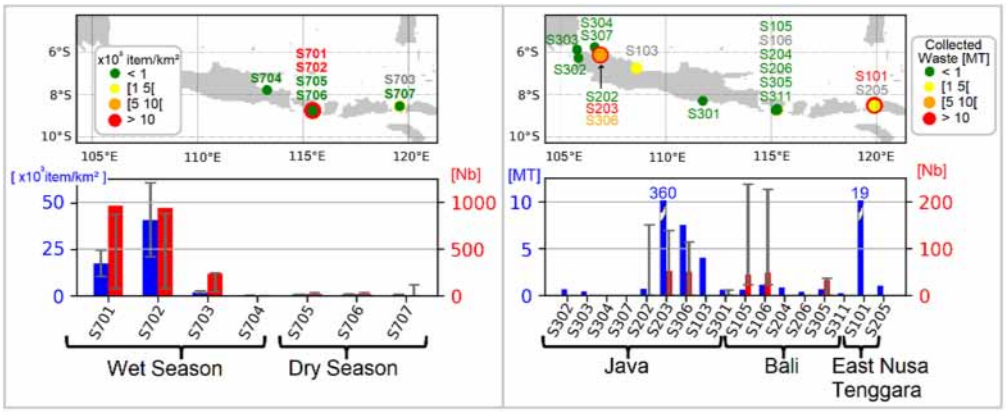

Figure 8. Comparison between our numerical simulation and observations from (**left panel**) cleaning sessions presented by [43] at the APEC Bali workshop and (**right panel**) visual surveys presented in [41]. In the left panels, the units are in metric tons (MT), and in the right panels, units are in 10^3 *item*/km^2. Maps in the upper row show the different site locations. Bar plots in the lower row show in situ observations (in blue, left ordinate axis) vs. simulation results (in red, right ordinate axis). In the lower left (respectively, Right) panel, simulation results are computed as the number of particles stranded within a 20 km range from the site location and during the 7 (respectively, 60) days prior to the cleaning session (respectively, end of the visual survey). For simulation results, grey error lines illustrate the 5th and 95th percentiles of the number of stranded particles that were computed considering slight changes in time (plus or minus 7 days around the cleaning session date or minus 30 days from the end of the visual survey) and position (10 km range from the site location). For observation results, grey error lines illustrate the study error, when available.

The second set of comparisons was performed using observations from PS. The purpose of the PS study was not to compare the relative amounts of waste between monsoons but to clean beaches and estimate the weight of the waste collected. It appears that, apart from on Bali, no beaches were cleaned during both the wet and dry seasons; thus, the monsoonal variability in strandings could not be compared in this case. The correlation between the simulation and observations was not as striking as with the GS dataset (lower right panel of Figure 8), and the specific conditions of each site need to be analyzed.

Most sites on Java Island (S301, S302, S303, S304 and S307) reported low collected weights (616, 668, 404, 69 and 10 kg, respectively) consistent with data showing no strandings in our simulations (0 [0-11], 0 [0-0], 0 [0-3], 4 [0-4], 0 [0-0] stranded particles, respectively; the numbers in square brackets indicate the corresponding 5th and 95th percentiles). The best concordances between collected waste and simulated strandings occurred for Jakarta sites S203 and S306, where both observation (12,000 and 7525 kg, respectively) and simulation (52 [0-138] and 50 [0-114] stranded particles, respectively) reported high rates of strandings. It should be noted that the Jakarta site S202 reported low collected weight (693 kg) and no simulated strandings (0 stranded particles); this is consistent, but the simulation error bar (0 to 150 stranded particles) suggests that the contrary could also have been found with a slight change in the location and sampling date. On the other hand, a large amount of waste was collected at site S103 (4000 kg), which was close to the densely populated city of Cirebon, whereas no stranding (0 [0-0]) occurred in our simulation. Indeed, in the simulation, no riverine source was selected close to Cirebon, and the oceanic currents used in the model did not allow particles from the nearby Ciliwung, Citarum and Cisadane rivers to drift and strand along this part of the coast (Figure 4). This suggests that the pollution at site S103 was locally sourced and that the source scenario of the simulation should be upgraded.

All sites located on Bali (S105, S106, S204, S206, S305 and S311) reported low collected weights (600, 1122, 841, 366 and 228 kg, respectively), whereas the simulated strandings reached high values for sites S105 and S106 (44 [22-237] and 48 [22-226] stranded particles, respectively) and, to a lesser extent, for site S305 (33 [0-36] stranded particles). The Bali sites were sampled in November 2017 (S105 and S106), September 2018 (S204), October 2018 (S206), May 2019 (S305) and December 2019 (S311). These Bali sites are highly touristic, and earlier cleanings of these sites might have biased the comparison. In support of this assumption, a *Guardian* article dated 4 January 2021 reported that the Kuta beach on Bali suffered a heavy pollution event in early 2021, with 30 to 60 tons of waste collected each day [49]. Although this *Guardian* article mentioned that this pollution event was recurrent during this period of the year, the waste collected on Bali's beaches never reached this intensity in the PS data.

On East Nusa Tenggara, there was a huge amount of waste collected at site S101 (10,001 kg), which was located close to the city of Labuan Bajo, whereas no simulated strandings occurred (0 [0-0]). In the simulation, no pollution source was selected close to this location. Site S101 was located in the small city of Labuan Bajo, which is a hub for accessing the Komodo Island touristic area. The city concentrates a high density of hotels and homestays for transiting tourists, with limited infrastructure for the collection of generated waste. The beach cleaning session took place at the harbor close to the mooring location of the Ferryboat. The pollution may accordingly be local and not considered in our source scenario. Low collected weights (1007 kg) were reported at site S205, consistent with the lack of simulated strandings (0 [0-0]). Site S205 was located in the same area as site S101, but the cleaning session took place the following year (in 2018). Thus, as for site S101, a pollution source was probably missing, and the comparison may be inadequate.

4. Discussion

The advection of numerical particles originating from 21 riverine sources in Indonesia showed that 60% of the particles stranded along the coasts inside the regional area, whereas

30% drifted away, mostly into the south Indian Ocean. The simulation also showed that particles tend to strand close in space and time to their riverine source. However, variabilities related to local ocean dynamical processes, local topography and coastline shapes exist. Sometimes, stranded particles originate from more remote sources than average or travel for a longer time in nearby water before stranding.

A strong seasonal signal of particle strandings was also revealed, with two seasonal peaks: one centered on January-February and one on June-July. This seasonality is linked to the monsoon influence on both surface currents and river discharge. The strong seasonality of this pollution has already been emphasized in previous studies [41,50,51] and reported in press articles [49], and the peak periods in these different field observations match those in our simulation. Strandings decreased over the two last years of our simulation. Nevertheless, the time series was too short to correlate this decrease with interannual oscillations. A longer time series, including different phases of ENSO and IOD, deserves further attention in the future.

It is noteworthy that using a higher (respectively, lower) stranding threshold (i.e., the distance below which a particle is considered stranded) resulted in more (respectively, fewer) stranded particles being counted. However, the relative distribution of the stranded particles in time and space remained similar (not shown here).

The physical processes driving particle dispersion and stranding also require deeper investigation. Surface Stokes drift and tidal surface currents can have a strong influence on the fate of particles. We performed an initial influence assessment using supplementary sensitivity tests, including the removal of tidal currents and surface Stokes drift (results not shown here). Our results showed that the surface Stokes drift had a stronger impact in terms of regional dispersion and the number of particles stranded when compared to the contribution of tidal currents. However, simply adding the different surface current components, instead of coupling the different processes in numerical simulations, did not account for the existing interactions between tides and the topography or between the Stokes drift and the simple surface currents. Recent tide-coupled simulations have shown a significant impact of tides on debris dispersion and fate, with an increase in the number of particles stranded and some local variations when compared to the simple sum of tidal and surface currents [52]. On the other hand, the impact of surface Stokes drift can decrease because of its interaction with the mean flow through the anti-Stokes effect, as discussed in [47]. These couplings and interactions deserve further analyses.

The resolution of the model may also have influenced the simulated trajectories. In particular, we aimed to release particles inside the river plumes, but a 9 km grid may not be sufficient to correctly locate river plumes and their associated salinity fronts. Supplementary simulations are needed to assess the sensitivity of the results to the resolution of the model. These sensitivity tests to resolution are especially important as this first study shows that strandings mainly occur close to river sources.

Assessing the performance of strandings simulated by a numerical experiment proved to be complex, as mentioned in [53]. To assess this performance, we compared simulated stranding results with different datasets assembled based on observations. We encountered three main difficulties. Firstly, among the seven available field studies that have been evaluated [41,43,50,54–57], only two were sufficiently relevant to allow performing a comparison [41,43], for reasons that are explained in the following paragraph. Secondly, comparisons had to be conducted in a nuanced fashion depending on the particularities of each field study. Finally, the comparison results had to be interpreted with caution due to the limitations stemming from the simulation assumptions.

Concerning the choice of relevant field studies, we had to discard studies where crucial information was lacking. For instance, the exact sampling dates and sampling periods of the observations were missing in [41,54]; counting debris on a precise sampling date is of great importance, especially in Indonesia and more generally in South-East Asia, where the seasonal variability in strandings is pronounced. Furthermore, studies often focus on very specific areas; this drastically limits possible spatial comparisons with

numerical experiments. In [50,55–57], the sites were all located within surface areas that corresponded only to one or two grid cells of our numerical experiment. Finally, because of the limited spatial resolution of the model, the numerical coastal shape may hinder relevant comparisons (e.g., a site located inside a narrow strait might not be explicitly resolved by the present model).

We could not aggregate field data from different studies because field methods are numerous and rarely comparable: the cumulated times of observation, sampling methods, types of sampled sites and units often differ from one dataset to the other. In particular, for the datasets used in our study, the observations from the PS study were not homogenized to a surface area, and previous cleanings were not reported; in the GP study, the exact periods of sampling for observations were missing. Things are evolving; several protocols have been recently published to aid in the homogenization of plastic and waste measurements (e.g., [58–61]). Newly implemented studies tend to adopt a similar protocol [62], and future comparisons should be facilitated.

Concerning the simulation assumptions, the source scenario of our numerical experiment only accounted for Indonesian river sources, whereas other "real" sources co-exist in Indonesia and at the regional scale of the South China Sea. The comparison results revealed local discrepancies between the source scenario and observed pollution. For instance, a pollution source was probably missing from our source scenario close to the city of Cirebon (Java), which led to no simulated stranding, whereas a large amount of waste was collected during beach cleaning sessions. The source scenario should be upgraded in a future work to include missing sources.

For all these reasons, comparing simulation results with field observations remains a challenging task requiring a thorough examination of the methodology and results of each field study as well as the assumptions on which each simulation was built. The aforementioned limitations should be kept in mind when switching to global simulations and/or systematic comparisons with global databases [63].

Other means of Lagrangian performance assessment exist and may be worth considering. In particular, drifters' trajectories can be compared with simulated trajectories. However, comparisons with real trajectories should be interpreted with caution: they are often more sensitive to windage, a process that can significantly affect trajectories and that has not been accounted for in the present study. Adding more ocean physics, such as windage or the specific transformation of any one type of plastic, would represent another full study; such an endeavor definitely deserves more attention in the future. As an additional difficulty, very few drifters travel through the Indonesian seas. This fact drastically restricts a robust validation in this area, i.e., the existing drifter array from the Global Drifter Program. To assess the performance of simulated trajectories in the Indonesian seas, a few CLS drifters were released in the vicinity of river mouths. Initial performance assessments can be found in [64]. However, additional drifters are planned to be released to complete the time and space coverage that is needed to allow a relevant comparison with the model.

Author Contributions: Conceptualization, D.D. and C.M.; methodology, D.D., C.M., E.M., R.R., B.G.G., A.R.F. and E.D.; software, D.D.; validation, D.D.; formal analysis, D.D.; writing—original draft preparation, D.D.; writing—review and editing, C.M., E.M., R.R., B.G.G., A.R.F. and E.D.; visualization, D.D.; supervision, C.M.; project administration, C.M. and E.D.; funding acquisition, C.M. and E.M. All authors have read and agreed to the published version of the manuscript.

Funding: This work was supported by the Agence Française de Développement (AFD) under the framework of a Fund for Technical Expertise and Experience Transfers (FEXTE), which supports technical cooperation programs and project-preparation studies.

Institutional Review Board Statement: Not applicable.

Informed Consent Statement: Not applicable.

Data Availability Statement: https://doi.org/10.12770/8dea4c5c-f2c2-4771-9372-9ce60c878c49, accessed on 9 June 2022.

Acknowledgments: We would like to thank Nicolas Grima and Bruno Blanke from the LOPS for providing the Ariane Lagrangian software package and updates to match the needs of the present study, as well as the two anonymous reviewers. We also thank Sapta Putra Ginting and his collaborators for agreeing to let us use the dataset they presented at the APEC Bali meeting about the waste collected during their beach cleaning sessions. This study benefitted from the support of the French National Research Institute for Sustainable Development (IRD).

Conflicts of Interest: The authors declare no conflict of interest.

References

1. Plastics Europe. Plastics, the Facts 2020. Available online: https://issuu.com/plasticseuropeebook/docs/plastics_the_facts-web-dec2020 (accessed on 16 February 2021).
2. Jambeck, J.R.; Geyer, R.; Wilcox, C.; Siegler, T.R.; Perryman, M.; Andrady, A.; Narayan, R.; Law, K.L. Plastic waste inputs from land into the ocean. *Science* **2015**, *347*, 768–771. [CrossRef] [PubMed]
3. Lebreton, L.; van der Zwet, J.; Damsteeg, J.W.; Slat, B.; Andrady, A.; Reisser, J. River plastic emissions to the world's oceans. *Nat. Commun.* **2017**, *8*, 15611. [CrossRef] [PubMed]
4. Alshawafi, A.; Analla, M.; Alwashali, E.; Ahechti, M.; Aksissou, M. Impacts of marine waste, ingestion of microplastic in the fish, impact on fishing yield, M'diq, Morocco. *Int. J. Mar. Biol. Res.* **2018**, *3*, 1–14. [CrossRef]
5. Fossi, M.C.; Panti, C.; Baini, M.; Lavers, J.L. A Review of Plastic-Associated Pressures: Cetaceans of the Mediterranean Sea and Eastern Australian Shearwaters as Case Studies. *Front. Mar. Sci.* **2018**, *5*, 173. [CrossRef]
6. Coppock, R.L.; Galloway, T.S.; Cole, M.; Fileman, E.S.; Queirós, A.M.; Lindeque, P.K. Microplastics alter feeding selectivity and faecal density in the copepod, Calanus helgolandicus. *Sci. Total Environ.* **2019**, *687*, 780–789. [CrossRef]
7. McIlgorm, A.; Campbell, H.F.; Rule, M.J. The economic cost and control of marine debris damage in the Asia-Pacific region. *Ocean Coast. Manag.* **2011**, *54*, 643–651. [CrossRef]
8. Jang, Y.C.; Hong, S.; Lee, J.; Lee, M.J.; Shim, W.J. Estimation of lost tourism revenue in Geoje Island from the 2011 marine debris pollution event in South Korea. *Mar. Pollut. Bull.* **2014**, *81*, 49–54. [CrossRef]
9. UNEP. Marine Plastic Debris and Microplastics: Global Lessons and Research to Inspire Action and Guide Policy Change. United Nations Environment Programme, 2016, 274p. Available online: https://wedocs.unep.org/20.500.11822/7720 (accessed on 9 June 2022).
10. Uddin, S.; Fowler, S.W.; Behbehani, M. An assessment of microplastic inputs into the aquatic environment from wastewater streams. *Mar. Pollut. Bull.* **2020**, *160*, 111538. [CrossRef]
11. Martinez, E.; Maamaatuaiahutapu, K.; Taillandier, V. Floating marine debris surface drift: Convergence and accumulation toward the South Pacific subtropical gyre. *Mar. Pollut. Bull.* **2009**, *58*, 1347–1355. [CrossRef]
12. Maximenko, N.; Hafner, J.; Niiler, P. Pathways of marine debris derived from trajectories of Lagrangian drifters. *Mar. Pollut. Bull.* **2012**, *65*, 51–62. [CrossRef]
13. van Sebille, E.; England, M.H.; Froyland, G. Origin, dynamics and evolution of ocean garbage patches from observed surface drifters. *Environ. Res. Lett.* **2012**, *7*, 044040. [CrossRef]
14. Maes, C.; Grima, N.; Blanke, B.; Martinez, E.; Paviet-Salomon, T.; Huck, T. A Surface "Superconvergence" Pathway Connecting the South Indian Ocean to the Subtropical South Pacific Gyre. *Geophys. Res. Lett.* **2018**, *45*, 1915–1922. [CrossRef]
15. Fazey, F.M.; Ryan, P.G. Biofouling on buoyant marine plastics: An experimental study into the effect of size on surface longevity. *Environ. Pollut.* **2016**, *210*, 354–360. [CrossRef] [PubMed]
16. Lobelle, D.; Kooi, M.; Koelmans, A.A.; Laufkötter, C.; Jongedijk, C.E.; Kehl, C.; van Sebille, E. Global modeled sinking characteristics of biofouled microplastic. *J. Geophys. Res. Oceans* **2021**, *126*, e2020JC017098. [CrossRef] [PubMed]
17. Maes, C.; Blanke, B. Tracking the origins of plastic debris across the Coral Sea: A case study from the Ouvéa Island, New Caledonia. *Mar. Pollut. Bull.* **2015**, *97*, 160–168. [CrossRef]
18. Onink, V.; Jongedijk, C.E.; Hoffman, M.J.; van Sebille, E.; Laufkötter, C. Global simulations of marine plastic transport show plastic trapping in coastal zones. *Environ. Res. Lett.* **2021**, *16*, 064053. [CrossRef]
19. Chenillat, F.; Huck, T.; Maes, C.; Grima, N.; Blanke, B. Fate of floating plastic debris released along the coasts in a global ocean model. *Mar. Pollut. Bull.* **2021**, *165*, 112–116. [CrossRef]
20. Weiss, L.; Ludwig, W.; Heussner, S.; Canals, M.; Ghiglione, J.F.; Estournel, C.; Constant, M.; Kerhervé, P. The missing ocean plastic sink: Gone with the rivers. *Science* **2021**, *373*, 107–111. [CrossRef]
21. Center for International Earth Science Information Network—CIESIN—Columbia University. Gridded Population of the World, Version 4 (GPWv4): Population Density, Revision 11. Palisades, NY: NASA Socioeconomic Data and Applications Center (SEDAC). 2018. Available online: https://sedac.ciesin.columbia.edu/data/set/gpw-v4-population-density-rev11 (accessed on 5 August 2020).
22. ERA5. ERA5 Hourly Data on Single Levels from 1979 to Present. Available online: https://cds.climate.copernicus.eu/cdsapp#!/dataset/reanalysis-era5-single-levels?tab=form (accessed on 17 September 2020).
23. Andréfouët, S.; Paul, M.; Farhan, A.R. Indonesia's 13558 islands: A new census from space and a first step towards a One Map for Small Islands Policy. *Mar. Policy* **2022**, *135*, 104848. [CrossRef]

24. Ministry of Environment and Forestry. National Plastic Waste Reduction Strategic Actions for Indonesia, Republic of Indonesia. 2020. Available online: https://www.unenvironment.org/ietc/resources/policy-and-strategy/national-plastic-waste-reduction-strategic-actions-indonesia (accessed on 9 June 2022).
25. Fraser, C.; Morrison, A.; Hogg, A.; Macaya, E.; Van Sebille, E.; Ryan, P.; Padovan, A.; Jack, C.; Valdivia, N.; Waters, J.M. Antarctica's ecological isolation will be broken by storm-driven dispersal and warming. *Nat. Clim. Chang.* **2016**, *8*, 704–708. [CrossRef]
26. Dobler, D.; Huck, T.; Maes, C.; Grima, N.; Blanke, B.; Martinez, E.; Ardhuin, F. Large impact of Stokes drift on the fate of surface floating debris in the South Indian Basin. *Mar. Pollut. Bull.* **2019**, *148*, 202–209. [CrossRef] [PubMed]
27. Pujiana, K.; McPhaden, M.J. Intraseasonal Kelvin Waves in the Equatorial Indian Ocean and Their Propagation into the Indonesian Seas. *J. Geophys. Res. Oceans* **2020**, *125*, e2019JC015839. [CrossRef]
28. Rothstein, L.M.; McPhaden, M.J.; Proehl, J.A. Wind Forced Wave-Mean Flow Interactions in the Equatorial Waveguide. Part I: The Kelvin Wave. *J. Phys. Oceanogr.* **1988**, *18*, 1435–1447. [CrossRef]
29. Wyrtki, K. *Physical Oceanography of the Southeast Asian Waters*; NAGA REPORT 2; Scripps Institution of Oceanography: San Diego, CA, USA, 1961; 195p.
30. Ray, R.D.; Egbert, G.D.; Erofeeva, S.Y. A Brief Overview of Tides in the Indonesian Seas. *Oceanography* **2005**, *18*, 74–79. [CrossRef]
31. Haryanto, B.; Lestari, F.; Nurlambang, T. Extreme Events, Disasters, and Health Impacts in Indonesia. In *Extreme Weather Events and Human Health*; Akhtar, R., Ed.; Springer: Cham, Switzerland, 2020; pp. 227–245. [CrossRef]
32. Kerry, E. Tropical Cyclones. *Annu. Rev. Earth Planet. Sci.* **2003**, *31*, 75–104. [CrossRef]
33. Gordon, A.L.; Huber, B.A.; Metzger, E.J.; Susanto, R.D.; Hurlburt, H.E.; Adi, T.R. South China Sea throughflow impact on the Indonesian throughflow. *Geophys. Res. Lett.* **2012**, *39*, L11602. [CrossRef]
34. Sprintall, J.; Gordon, A.L.; Wijffels, S.E.; Feng, M.; Hu, S.; Koch-Larrouy, A.; Phillips, H.; Nugroho, D.; Napitu, A.; Pujiana, K.; et al. Detecting Change in the Indonesian Seas. *Front. Mar. Sci.* **2019**, *6*, 257. [CrossRef]
35. Dobler, D.; Martinez, E.; Rahmania, R.; Gautama, B.G.; Farhan, A.R.; Maes, C. *Floating Marine Debris along Indonesian Coasts: An Atlas of Strandings Based on Lagrangian Modelling*; "Monitoring and Modelling the Circulation of Marine Debris in Indonesia" Project Funded by AFD; IRD: Jakarta, Indonesia, 2021; 92p.
36. SMOC. Global Ocean 1/12° Physics Analysis and Forecast Updated Daily. Available online: https://resources.marine.copernicus.eu/product-detail/GLOBAL_ANALYSIS_FORECAST_PHY_001_024/DOCUMENTATION (accessed on 5 June 2020).
37. Dai, A.; Qian, T.; Trenberth, K.E.; Milliman, J.D. Changes in continental freshwater discharge from 1948–2004. *J. Clim.* **2009**, *22*, 2773–2791. [CrossRef]
38. Liu, Y.; Weisberg, R.H. Evaluation of trajectory modeling in different dynamic regions using normalized cumulative Lagrangian separation. *J. Geophys. Res. Oceans* **2011**, *116*, C9. [CrossRef]
39. Révelard, A.; Reyes, E.; Mourre, B.; Hernández-Carrasco, I.; Rubio, A.; Lorente, P.; Fernández, C.D.L.; Mader, J.; Álvarez Fanjul, E.; Tintoré, J. Sensitivity of skill score metric to validate Lagrangian simulations in coastal areas: Recommendations for search and rescue applications. *Front. Mar. Sci.* **2021**, *8*, 630388. [CrossRef]
40. GloFAS. River Discharge and Related Historical Data from the Global Flood Awareness System (GloFAS). Available online: https://cds.climate.copernicus.eu/cdsapp#!/dataset/cems-glofas-historical?tab=form (accessed on 18 September 2020).
41. Germanov, E.S.; Marshall, A.D.; Hendrawan, I.G.; Admiraal, R.; Rohner, C.A.; Argeswara, J.; Wulandari, R.; Himawan, M.R.; Loneragan, N.R. Microplastics on the Menu: Plastics Pollute Indonesian Manta Ray and Whale Shark Feeding Grounds. *Front. Mar. Sci.* **2019**, *6*, 679. [CrossRef]
42. APEC Ocean and Fisheries Working Group. Capacity Building on Global Marine Debris Monitoring and Modeling: Supports Protection of the Marine Environment. Published under SOM Steering Committee on Economic and Technical Cooperation (SCE) and Ocean and Fisheries Working Group (OFWG). In Proceedings of the APEC Bali Workshop, Bali, Indonesia, 18–20 February 2020. Available online: https://www.apec.org/publications/2020/06/capacity-building-on-global-marine-debris-monitoring-and-modeling (accessed on 9 June 2022).
43. Putra, S. Initiatives MMAF on Reducing Marine Debris. In Proceedings of the APEC Bali Workshop, Bali, Indonesia, 18–20 February 2020. Available online: https://tinyurl.com/3vfzz8x2 (accessed on 9 June 2022).
44. van Sebille, E.; Griffies, S.M.; Abernathey, R.; Adams, T.P.; Berloff, P.; Biastoch, A.; Blanke, B.; Chassignet, E.P.; Cheng, Y.; Cotter, C.J.; et al. Lagrangian ocean analysis: Fundamentals and practices. *Ocean Model.* **2018**, *121*, 49–75. [CrossRef]
45. Blanke, B.; Raynaud, S. Kinematics of the Pacific Equatorial Undercurrent: An Eulerian and Lagrangian approach from GCM results. *J. Phys. Oceanogr.* **1997**, *27*, 1038–1053. [CrossRef]
46. van Emmerik, T.; Mellink, Y.; Hauk, R.; Waldschläger, K.; Schreyers, L. Rivers as Plastic Reservoirs. *Front. Water* **2022**, *3*, 786936. [CrossRef]
47. van Sebille, E.; Aliani, S.; Law, K.L.; Maximenko, N.; Alsina, J.M.; Bagaev, A.; Blanke, B.; Chassignet, E.P.; Cheng, Y.; Cotter, C.J.; et al. The physical oceanography of the transport of floating marine debris. *Environ. Res. Lett.* **2020**, *15*, 023003. [CrossRef]
48. van der Mheen, M.; van Sebille, E.; Pattiaratchi, C. Beaching patterns of plastic debris along the Indian Ocean rim. *Ocean Sci.* **2020**, *16*, 1317–1336. [CrossRef]
49. The Guardian. Bali's Beaches Buried in Tide of Plastic Rubbish during Monsoon Season. 2021. Available online: https://www.theguardian.com/world/2021/jan/04/balis-beaches-buried-in-tide-of-plastic-rubbish-as-monsoon (accessed on 9 June 2022).

50. Suteja, Y.; Atmadipoera, A.S.; Riani, E.; Nurjaya, I.W.; Nugroho, D.; Purwiyanto, A.I.S. Stranded marine debris on the touristic beaches in the south of Bali Island, Indonesia: The spatiotemporal abundance and characteristic. *Mar. Pollut. Bull.* **2021**, *173*, 113026. [CrossRef]
51. Phelan, A.; Ross, H.; Setianto, N.A.; Fielding, K.; Pradipta, L. Ocean plastic crisis—Mental models of plastic pollution from remote Indonesian coastal communities. *PLoS ONE* **2020**, *15*, e0236149. [CrossRef]
52. Maes, C.; Dobler, D.; Bertin, S.; Martinez, E.; Rahmania, R.; Gautama, B.G.; Farhan, A.R.; Herrmann, M. Disentangling the physical dispersion of floating debris and plastics in the Indonesian seas. In Proceedings of the OCEANS 2021: San Diego—Porto, San Diego, CA, USA, 20–23 September 2021; pp. 1–9. [CrossRef]
53. Lavers, J.L.; Oppel, S.; Bond, A.L. Factors influencing the detection of beach plastic debris. *Mar. Environ. Res.* **2016**, *119*, 245–251. [CrossRef]
54. Syakti, A.D.; Jacob, M.; Birrien, T.; Suhana, M.P.; Aziz, M.Y.; Salim, A.; Doumenq, P.; Louarn, G. Daily apportionment of stranded plastic debris in the Bintan Coastal area, Indonesia. *Mar. Pollut. Bull.* **2019**, *149*, 110609. [CrossRef]
55. Syakti, A.D.; Bouhroum, R.; Hidayati, N.V.; Koenawan, C.J.; Boulkamh, A.; Sulistyo, I.; Lebarillier, S.; Akhlus, S.; Doumenq, P.; Wong-Wah-Chung, P. Beach macro-litter monitoring and floating microplastic in a coastal area of Indonesia. *Mar. Pollut. Bull.* **2017**, *122*, 217–225. [CrossRef]
56. Bangun, A.P.; Wahyuningsih, H.; Muhtadi, A. Impacts of macro—And microplastic on macrozoobenthos abundance in intertidal zone. *IOP Conf. Ser. Ser. Earth Environ. Sci.* **2018**, *122*, 012102. [CrossRef]
57. Tahir, A.; Werorilangi, S.; Isman, F.; Zulkarnaen, A.; Massinai, A.; Faizal, A. Short-term observation on marine debris at coastal areas of Takalar District and Makassar City, South Sulawesi-Indonesia. *J. Ilmu Kelaut. SPERMONDE* **2019**, *4*, 48–53. [CrossRef]
58. MSFD Marine Litter Group. Guidance on Monitoring of Marine Litter in European Seas. Joint Research Centre of the European Commission. 2013. Technical Report. Available online: http://publications.jrc.ec.europa.eu/repository/bitstream/JRC83985/lb-na-26113-en-n.pdf (accessed on 9 June 2022).
59. Vlachogianni, T.; Paraskevopoulou, V.; Kalampokis, V.; Palatinus, A.; Trdan, S.; Muccio, S.D.; Alcaro, L.; Ronchi, F.; Mazziotti, C.; Zeri, C.; et al. Methodology for Monitoring Marine Litter on Beaches. DeFishGear Project, 2017. Technical Report, 16p. Available online: https://mio-ecsde.org/wp-content/uploads/2017/11/Beach-litter_monitoring-methodology.pdf (accessed on 9 June 2022).
60. Lacroix, C.; Kerambrun, L. Développement d'un Protocole de Suivi des Microparticules sur le Littoral de France Métropolitaine dans le Cadre du Programme de Surveillance DCSMM. CEDRE, AFB, 2018. Technical Report, 125p. Available online: https://doc.cedre.fr/index.php?lvl=notice_display&id=9797 (accessed on 9 June 2022).
61. Yutaka, M.; Chavanich, S.; Cabañas, A.C.; Hagmann, P.; Hinata, H.; Isobe, A.; Kershaw, P.; Kozlovskii, N.; Li, D.; Lusher, A.L.; et al. *Guidelines for Harmonizing Ocean Surface Microplastic Monitoring Methods*; Ministry of the Environment Japan: Tokyo, Japan, 2019; 71p.
62. Isobe, A.; Azuma, T.; Cordova, M.R.; Cózar, A.; Galgani, F.; Hagita, R.; Kanhai, L.D.; Imai, K.; Iwasaki, S.; Kako, S.; et al. A multilevel dataset of microplastic abundance in the world's upper ocean and the Laurentian Great Lakes. *Microplastics Nanoplastics* **2021**, *1*, 16. [CrossRef]
63. Maximenko, N.; Corradi, P.; Law, K.L.; Van Sebille, E.; Garaba, S.P.; Lampitt, R.S.; Galgani, F.; Martinez-Vicente, V.; Goddijn-Murphy, L.; Veiga, J.M.; et al. Toward the integrated marine debris observing system. *Front. Mar. Sci.* **2019**, *6*, 447. [CrossRef]
64. Gautama, B.G.; Rizal, A.; Rahmania, R.; Farhan, A.R.; Berlianty, D.; Priyono, B.; Siong, K.; Harjono, M.R.; Voisin, J.B.; Maes, C.; et al. Forecasting the stranded area of marine debris in Indonesian coasts using mobidrift model and floating drifter. *IOP Conf. Ser. Earth Environ. Sci.* **2022**, *1033*, 012039. [CrossRef]